Fault Coverage Improvement of CMOS Analog Circuits Using Supply Current Testing Method

Abderrazak Arabi, Mouloud Ayad, Mourad Benziane, Nacerdine Bourouba and Abdesslam Belaout

***Abstract*— In this paper, a testing technique based on supply current verifying is presented, for fault detection of analog circuits containing CMOS operational amplifiers. This testing technique is employed and developed to maximize the fault coverage of the circuit under test (CUT) using transient and frequency responses of the supply current. This testing method is based on the over-sighting of the quiescent supply current (I_{ddq}) of the CMOS operational amplifier operating in its quiescent mode and the supply current of the CMOS operational amplifier used as a Sallen-Key band pass filter in the AC and transient operating domains. The faults investigated in our study are of bridging and open circuit types that occur at the CMOS transistor level. The Pspice software was used for the CUT simulation by applying Monte-Carlo analysis in faulty and fault free conditions. Test parameters are extracted and selected to be used as input features of our classifier.**

***Index Terms*— Analog circuits, CMOS operational amplifier, fault coverage, supply current.**

Original Research Paper
DOI: 10.53314/ELS2327009A

I. Introduction

Due to their complex constitution, fault detection, location and identification in analog and mixed circuits become more difficult. This difficulty is caused by the limitation of the outputs, inputs and testing signals on one hand. On the other hand, the manufacture of integrated circuits follows several technological processes such as oxidation, photolithography, etching, ion implantation and metallization, which are not immune to imperfections. This is said because of the exposure of this process to interfering anomalies which consequently in deliberately provokes the degradation of circuit performance [1]. Due to these problems, fault diagnosis and testing of analog circuits become the most bothersome tasks in designing and fabrication of integrated circuits [2]-[4].

Fault diagnosis methods are generally classified as simulation before test (SBT) and simulation after test (SAT) approaches [5]. Simulation before testing method uses fault dictionary methods or approximation methods to locate both catastrophic and parametric faults. Simulation after test approach performs fault diagnosis based on the simulation results obtained from measured responses or test variables. It is based on parameter identification and fault verification steps.

In CMOS integrated circuits, the most observed faults are catastrophic ones, such as bridges and open faults. These faults produce some changes in the topology of the circuit. Bridging faults can be resulted from undesired connections between the transistor nodes, whereas open faults are due to unconnected nodes of the transistor [6]. These kinds of fault are well monitored by both quiescent and transient current power supplies since they constitute elements of a low cost and high speed testing technique. Current monitoring based testing has proved effective for bridging fault types. Whereas, the open circuit defects usually provoke a delay in the transient current [7].

In the testing of analog CMOS circuits, many approaches have been proposed based on the verification of the quiescent supply current by implying different techniques as fault dictionary in [6], oscillations test technique in [8]-[10], assessment on its adequacy [11], IDDQ testing of low voltage [12] and novel built-in current-sensor [13]. However, some other testing methods have used a DC fault models for fault detection and isolation [14]-[17]. Besides, an AC approach that uses a phase difference between signals as an indicator for fault signature has been found to be successful for raising the fault coverage ratio for this kind of circuits [18].

This paper aims to improve the faults coverage of analog circuits containing CMOS operational amplifier (opamp). As a first attempt, the testing method is used to check the opamp operation in the quiescent and functional modes based on the frequency and the transient responses of the opamp supply current. Then, a fault classification step is realized based on machine learning classifiers using Matlab software. Input features of classifiers are extracted from frequency and transient responses of the supply current, where Monte Carlo analysis of Pspice software is used to generate testing data. This is to increase the fault coverage and improve the efficiency of the

Manuscript received 01 November 2022. Received in revised form 11 February 2023. Accepted for publication 27 March 2023.

Abderrazak Arabi is with the Institute of Optics and Precision Mechanics, and the LIS Laboratory, Faculty of Technology, Ferhat Abbas Setif 1 University, 19000, Setif, Algeria (phone: +213-659-51-59-25; e-mail: a.arabi@univ-setif.dz, arabi_abderrazak@yahoo.fr).

Mouloud Ayad is with the LPM3E Laboratory, Faculty of sciences and applied sciences, Bouira University, 10000, Bouira, Algeria (m.ayad@univ-bouira.dz).

Mourad Benziane is with the LPM3E Laboratory, Faculty of sciences and applied sciences, Bouira University, 10000, Bouira, Algeria (m.benziane@univ-bouira.dz).

Nacerdine Bourouba is with the LIS Laboratory, Faculty of Technology, Ferhat Abbas Setif 1 University, 19000, Setif, Algeria (e-mail: bourouband@yahoo.fr).

Abdeslam Belaout is with the LEPCI Laboratory, Faculty of Technology, Ferhat Abbas Setif 1 University, 19000, Setif, Algeria (e-mail: belaout_s@yahoo.fr).

proposed method. More details of our testing approach are discussed in section II.

II. Proposed testing methodology

Single catastrophic faults like bridging and open faults in two stages CMOS operational amplifier are considered for fault detection in this work. This amplifier circuit to be tested is shown in figure 1. The first phase of our method consists of carrying out the opamp test in its quiescent mode. The second test stage deals with the Sallen&Key band-pass active filter (see figure 2), built with this type of operational amplifiers and operating in frequency and transient modes. These circuits under test have been simulated using Orcad Pspice software. In the frequency domain, the CUTs are stimulated by an AC signal with an amplitude value of 5V. In contrast, a pulse signal with 5V peak amplitude, a 500µs pulse width and a period of 1ms is used as a stimuli signal in transient domain. In the case of opamp testing in quiescent mode, the input stimulus is applied to its positive input (IN+) and the negative input (IN-) is connected to the ground. In addition, bridging faults injected in these circuits are reported in table I and classified into 9 classes, these faults are modeled by a very small resistor value. Besides, open faults are presented in table II and classified into 15 classes, and they are modeled using a very high resistor value. Then, the CUT is simulated under Monte-Carlo analysis for 100 iterations using Pspice software for each class of faults [19].

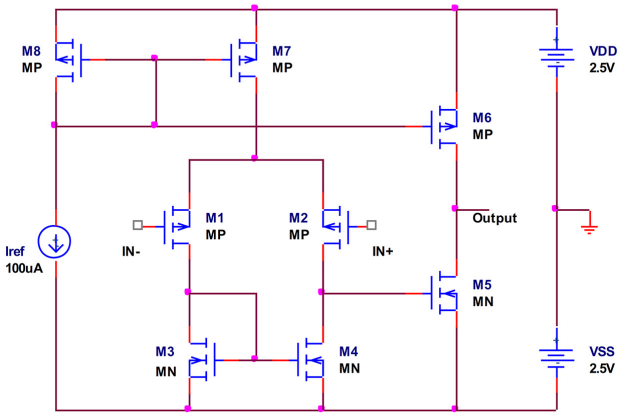

Fig. 1. Schematic of a two stages CMOS operational amplifier [1].

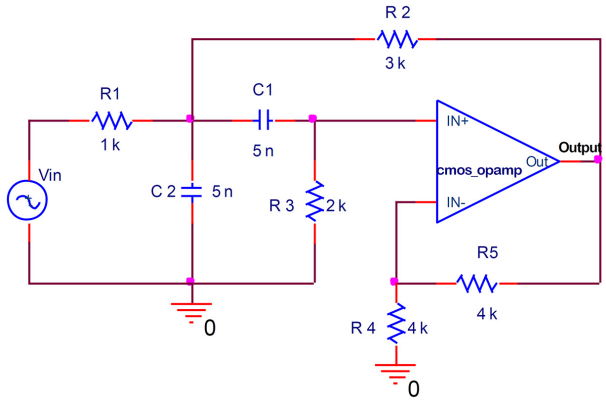

Fig. 2. Schematic of the band-pass active filter of Sallen&Key.

Table I
Catastrophic Bridging Faults

Fault code	Fault type	Affected transistor
F0	No Fault	-
F1	drain-source short	M3
F2	gate-drain short	M4
F3	drain-source short	M1
F4	drain-gate short	M2
F5	drain-gate short	M5
F6	gate-drain short	M6
F7	drain-source short	M6
F8	drain-source short	M7

Table II
Catastrophic open faults

Fault code	Fault type	Affected transistor
F0	No Fault	-
F1	Source open	M1
F2	Drain open	M1
F3	Drain open	M2
F4	Source open	M2
F5	Drain open	M3
F6	Gate open	M3
F7	Drain open	M4
F8	Gate open	M4
F9	Gate open	M5
F10	Drain open	M5
F11	Gate open	M6
F12	Gate open	M7
F13	Drain open	M8
F14	Gate open	M8

Figures 3 and 4 depict the frequency responses of the CMOS opamp supply current used in quiescent mode and in the Sallen-Key band pass filter configurations. While figures 5 and 6 illustrate the supply current transient responses of these two circuits respectively.

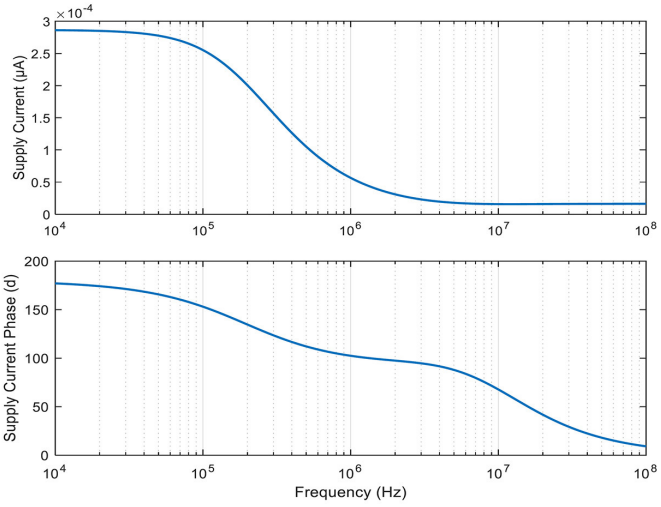

Fig. 3. Gain and phase of the quiescent supply current (IDDQ) of CMOS operational amplifier.

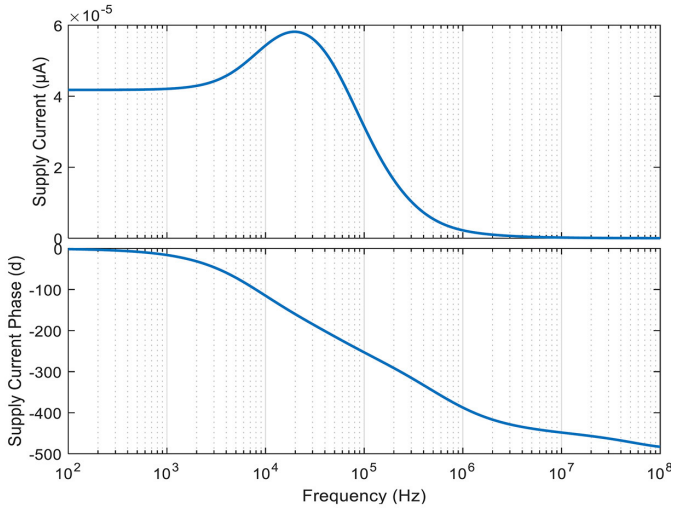

Fig. 4. Gain and phase of the opamp supply current in the Sallen-Key band-pass filter.

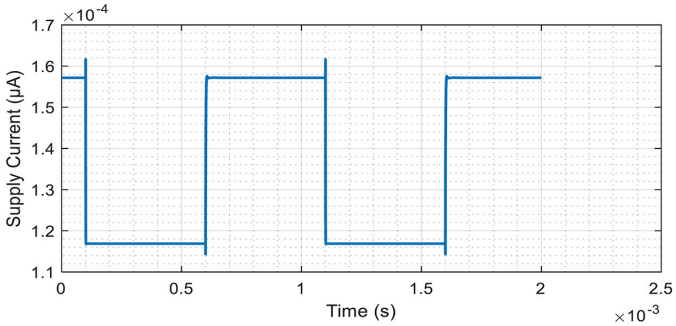

Fig. 5. Transient response of the opamp quiescent supply current.

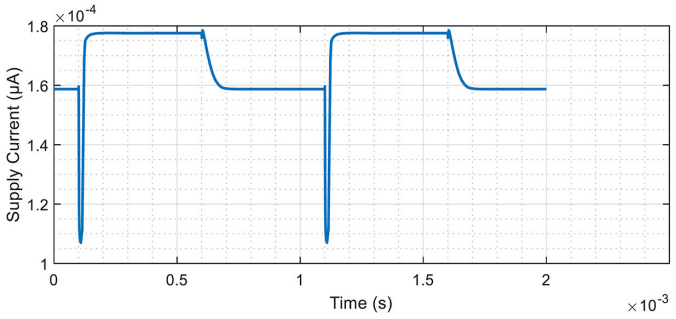

Fig. 6. Transient response of opamp supply current in the Sallen&Key band pass filter.

Regarding the CMOS operational amplifier circuit, the quiescent supply current and phase prove to be highly efficient in detecting of all bridging-type faults. Their illustration is highlighted in figure 7. However, for the open-circuit type faults, which are fourteen in number, their illustrative response curves are reduced to eight, one of which is that of the response in the absence of a fault, as illustrated in figure 8. This means the presence of ambiguous faults preventing their distinction between them.

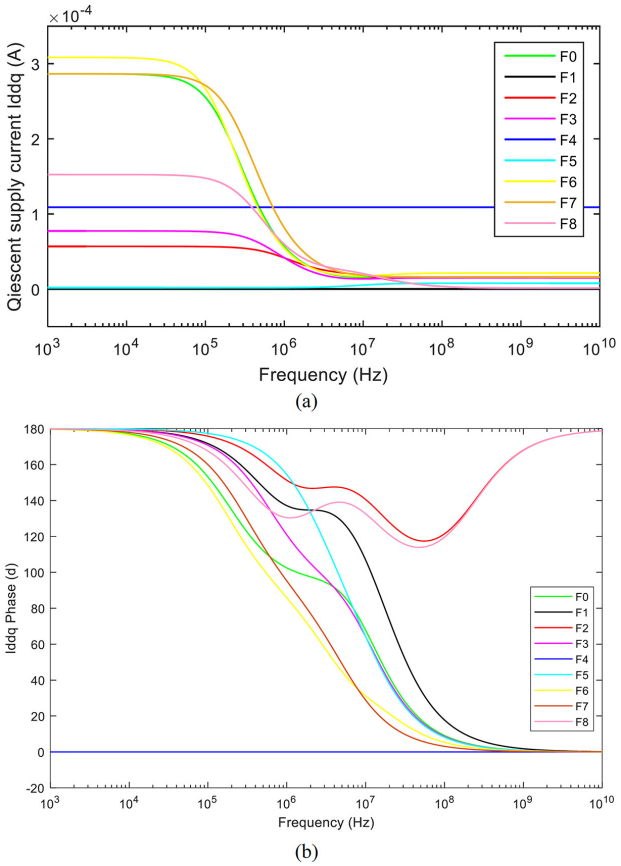

Fig. 7. Frequency responses of the of CMOS operational amplifier under bridging faults. (a): Quiescent supply current, (b): Supply current phase.

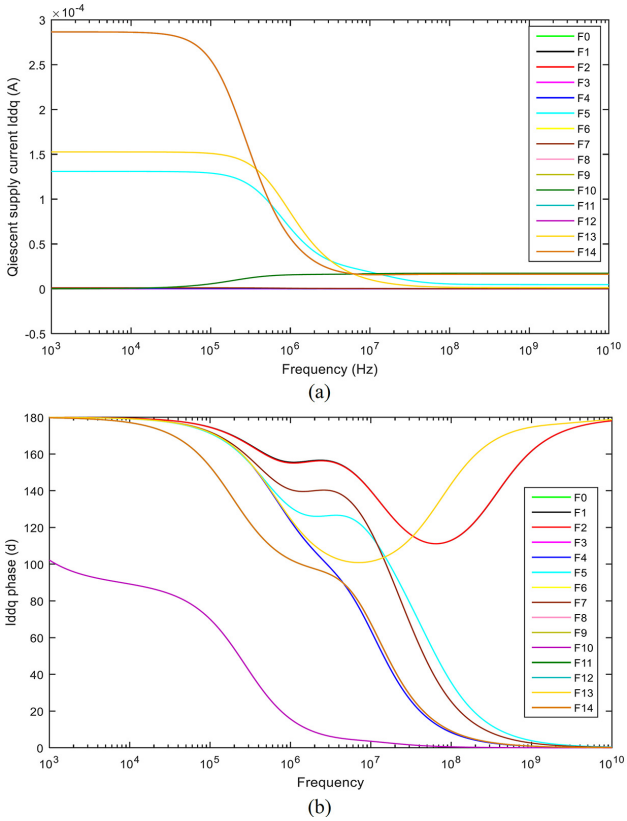

Fig. 8. Frequency responses of the of CMOS operational amplifier under open faults. (a): Quiescent supply current, (b): Supply current phase.

Exploration of Figures 9 and 10 shows the effectiveness of using the phase and amplitude of the supply current in the frequency domain chosen as parameters for detecting bridging faults for the Sallen-Key band pass filter circuit, as mentioned above subjected to this kind of investigation. The other highlight is the ambiguity of certain open faults despite their detection, are characterized by their curves almost superposed on each other that they are not distinguished.

To further improve the fault coverage process with less ambiguity and a high rate, the extracted parameters from the frequency and transient responses were introduced for the two aforementioned types of faults. This type of analysis concerns the responses in supply current and polarization of the two circuits under test, whose form of signals is illustrated by figures 11, 12, 13, and 14. This study emphasizes the extraction of useful features for the detection of bridging faults, with a total of 5 features identified. On the other hand, for the open circuit fault case, there are eight features extracted. This difference in number is due to the need for the fault coverage rate improvement that each type of faults requires.

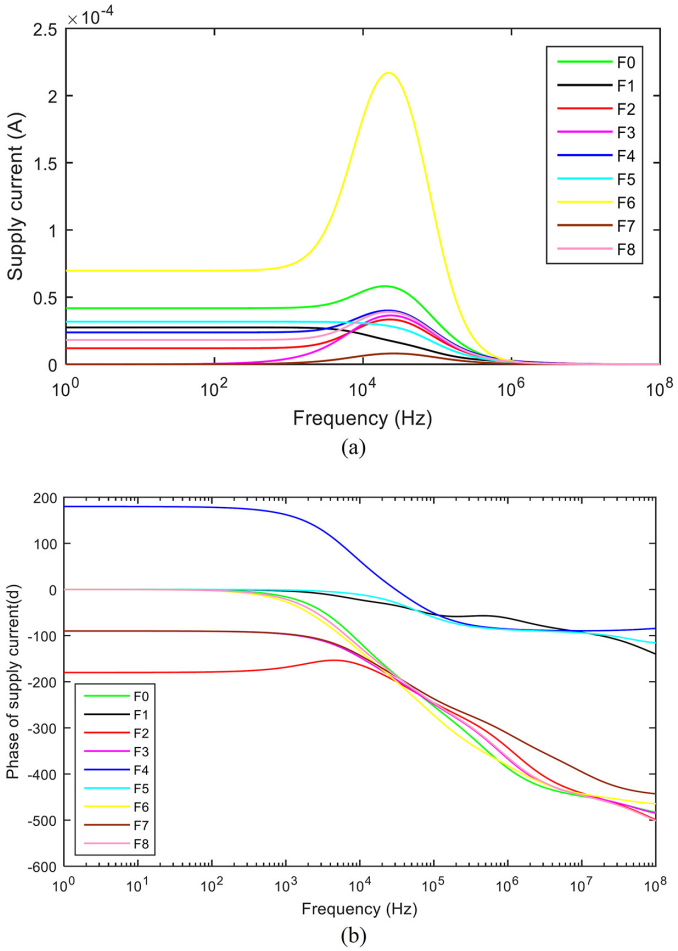

Fig. 9. Frequency responses of the Sallen&Key band-pass filter under bridging faults. (a): Supply current, (b): Supply current phase.

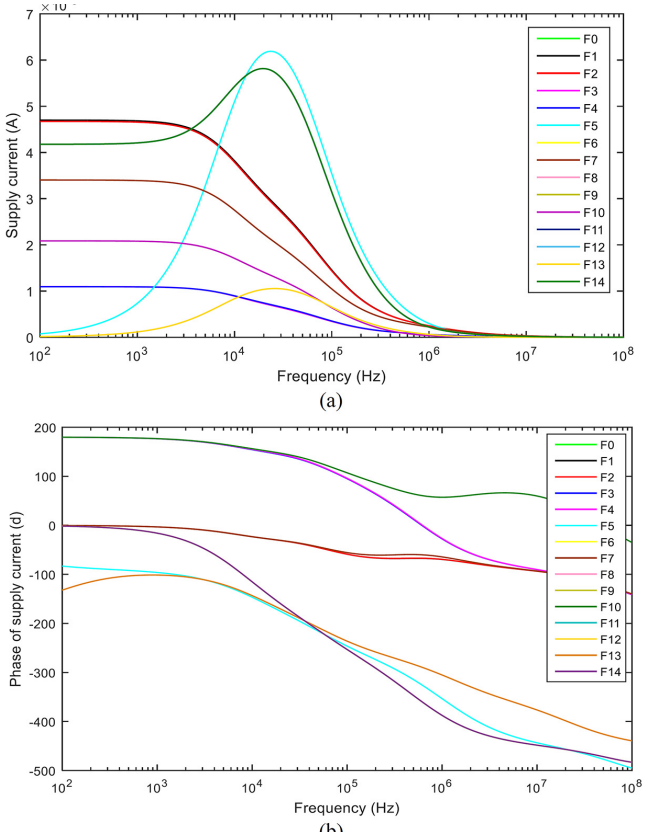

Fig. 10. Frequency responses of the Sallen&Key band-pass filter under open faults. (a): Supply current, (b): Supply current phase.

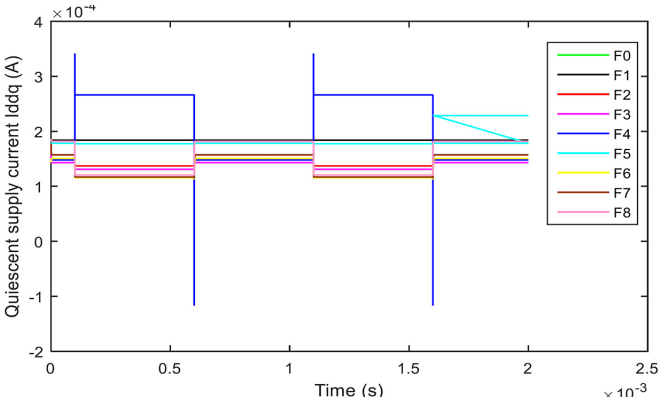

Fig. 11. Transient responses of quiescent supply current of the CMOS operational amplifier under bridging faults.

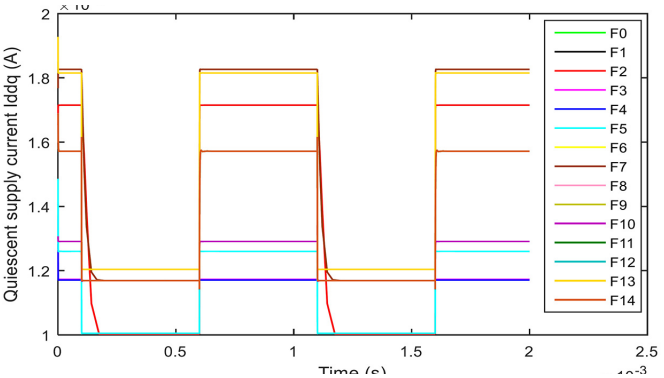

Fig. 12. Transient responses of quiescent supply current of the CMOS operational amplifier under open faults.

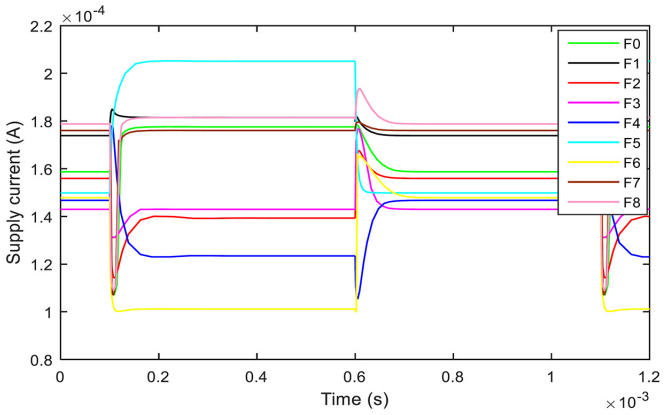

Fig. 13. Transient responses of opamp supply current in the Sallen&Key band-pass filter under bridging faults.

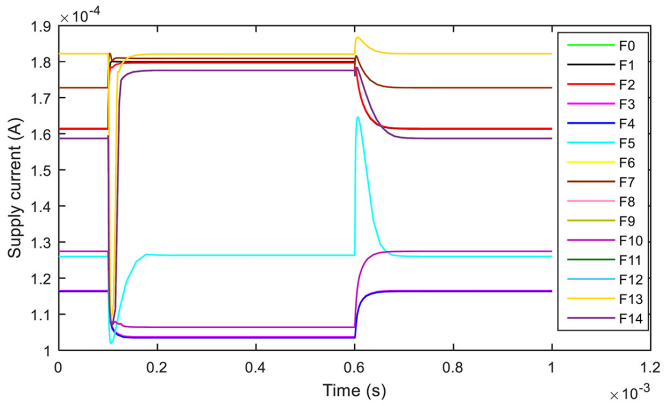

Fig. 14. Transient responses of the opamp supply current in the Sallen&Key band-pass filter under open faults.

A laborious work will acquire a volume of data on features to be treated and arranged for a better and more precise classification of faults. To achieve the desired results, the use of machine learning algorithms was unavoidable. This will serve to determine the classification accuracy for each fault class, using Matlab software. Further details of fault classification methodology are given in section III.

III. FAULT CLASSIFICATION

In this section, fault classification is done by using machine learning algorithms in Matlab software. First, the circuit under test is simulated using Monte Carlo analysis of Orcad pspice software for 100 iterations in both transient and frequency domains. Then, features are extracted from the obtained responses for each fault. Features values corresponding to fault free and faulty responses are collected in one matrix called fault-matrix. This matrix presents a database of our model to be used for proposed classifier training and testing. The different steps of the approach developed in this classifying process are illustrated in figure 15.

A. Classification of bridging faults

In this case, five features are extracted from the frequency and the transient responses of the supply current. Frequency features are peak amplitude, bandwidth, and center frequency, whereas transient ones are supply current maximal and minimal values of its transient response for fault free and faulty circuit conditions. These responses are illustrated in figures 16 and 17 successively.

In this case, the linear SVM classifier has given a classification accuracy of 100% for all considered bridging faults. The confusion matrix resulted from this classification is illustrated in figure 18.

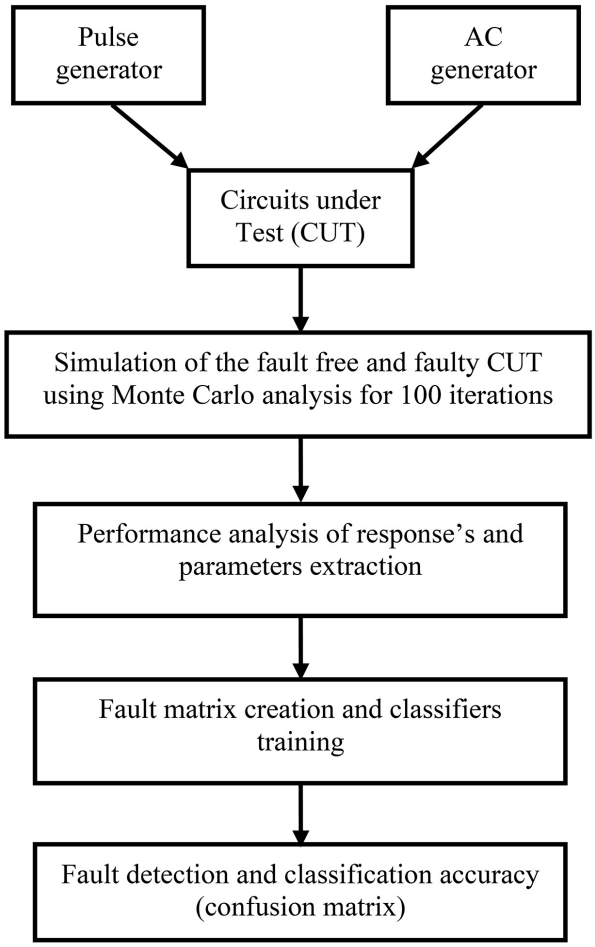

Fig. 15. Flow chart of the fault classification procedure.

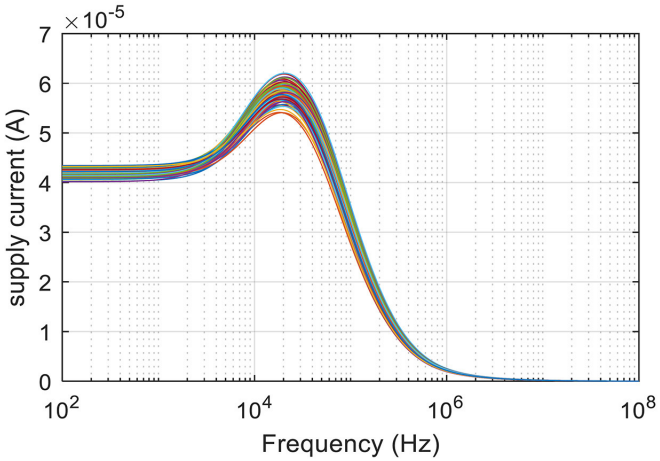

Fig. 16. Frequency responses of the supply current of the opamp in the Sallen&Key band-pass filter using Monte Carlo analysis.

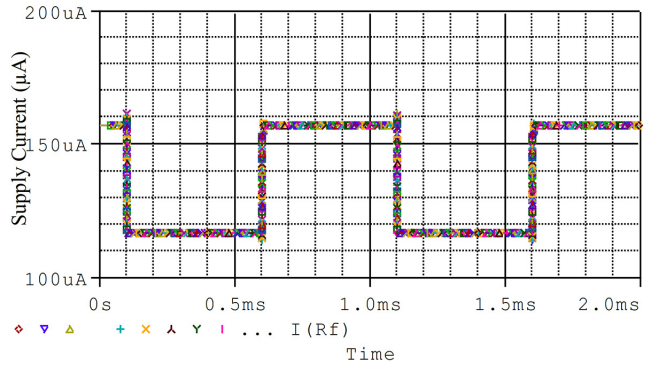

Fig. 17. Transient responses of the supply current of the opamp in the Sallen&Key band-pass filter using Monte Carlo analysis.

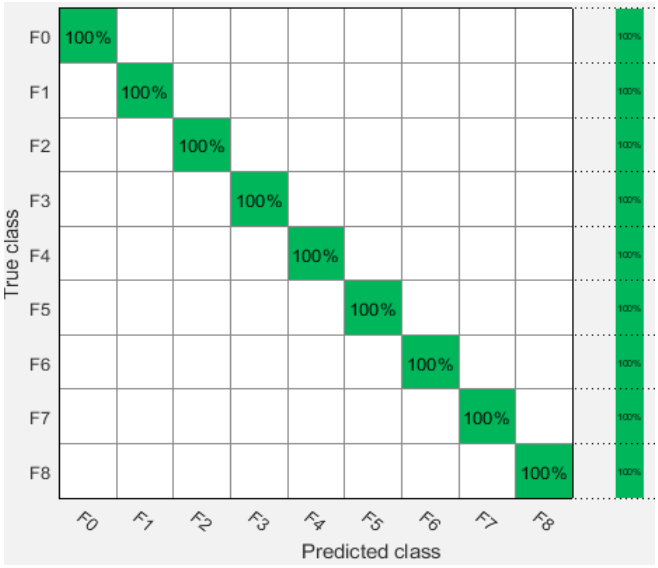

Fig. 18. Confusion matrix for linear SVM classifier.

B. Classification of open faults

In the open fault case, eight features are extracted from the frequency and the transient responses of the supply current signal. Frequency features correspond to the supply current maximal and minimal values and its phase maximal and minimal values as represented in figures 19 and 20. Moreover, the transient ones are maximal and minimal values, overshoot, and pulse width of the supply current transient responses for fault free and faulty cases (see figure 17). These features are named P1, P2, P3, P4, P5, P6, P7 and P8 respectively.

As far as a good classification accuracy for undetected faults are concerned and to make these distinguishable, three steps have been followed:

- Step 1: training all classifiers types of the classification learner tool with all input features, from which we select the best one that gives the highest classification accuracy.
- Step 2: re-training the best classifier having scored the higher classification accuracy in step 1 using only combinations of 4 optimized features. The remaining features are waived due to their low accuracy level. This features number reduction helps this classifier's accuracy to increase advantageously.

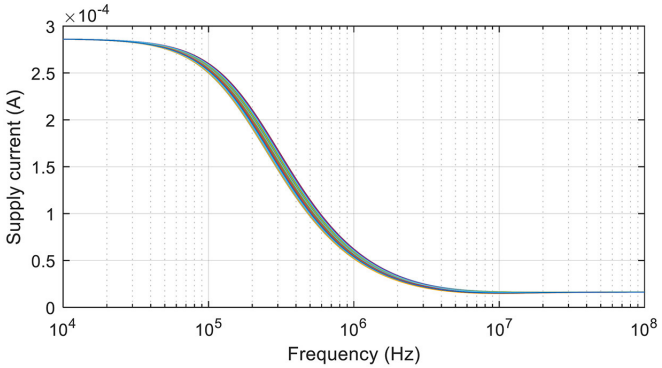

Fig. 19. Frequency responses of the CMOS opamp quiescent supply current using Monte Carlo simulation.

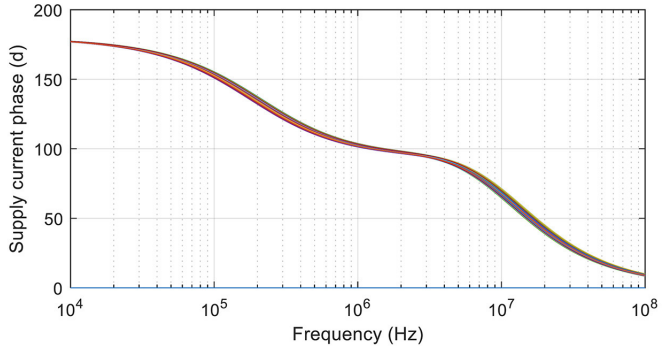

Fig. 20. Frequency responses of the supply current phase of the CMOS opamp using Monte Carlo simulation.

- Step 3: re-training the best classifier with the best combination of features and considering three validation cases: cross-validation, holdout validation, and no validation, using the classification learner tool.

From the result of the different fault classifiers we applied, the ones that give the best accuracy are: linear SVM classifier and weighted KNN classifier types, using three sorts of validation as mentioned in table V. These have led to the accuracy results with reduced parameters to a number of four and where the best one recorded with the weighted KNN is of 66.7% as summarized in table V. The corresponding confusion matrices exhibiting all the studied cases are shown in figures 21, 22, and 23.

However, other faults will be distinguished from each other using the confusion matrix parameters, leading to eliminating the ambiguity groups. These parameters are [20]-[21]:

- True positives of the class (TP): the number of good classed samples of the class (diagonal of the matrix).
- True negatives of the class (TN): the total number of TN is the sum of all columns and rows excluding that class's row and column.
- False positives of the class (FP): the total number of FP is the sum of values in the corresponding column of the class excluding its TP.
- False negatives (FN): the total number of FN is the sum of values in the corresponding row of the class excluding its TP.

The class's overall accuracy, precision, sensitivity, and specificity can be calculated from these parameters.

- Overall accuracy is calculated as the sum of the correct classifications divided by the total classes' number.

Precision: $$P = \frac{TP}{TP + FP} \quad (1)$$

Sensitivity: $$Se = \frac{TP}{TP + FN} \quad (2)$$

Specificity: $$Sp = \frac{TN}{TN + FP} \quad (3)$$

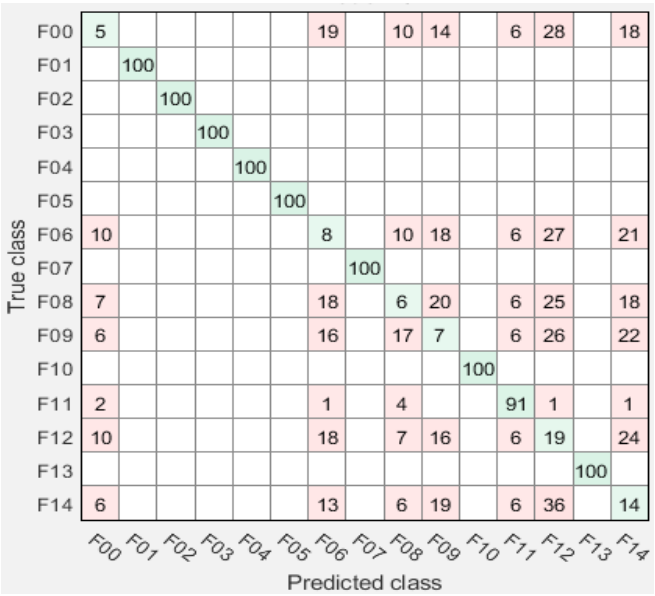

Fig. 21. Confusion matrix of Linear svm classifier with cross validation.

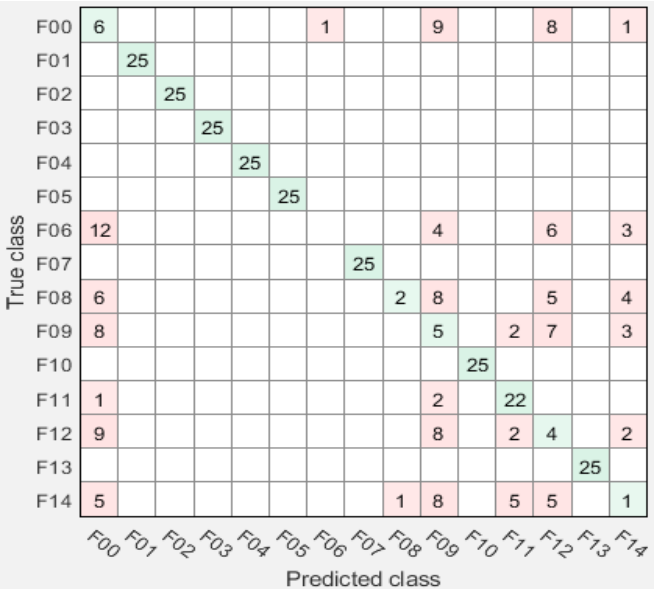

Fig. 22. Confusion matrix of linear svm classifier with holdout validation.

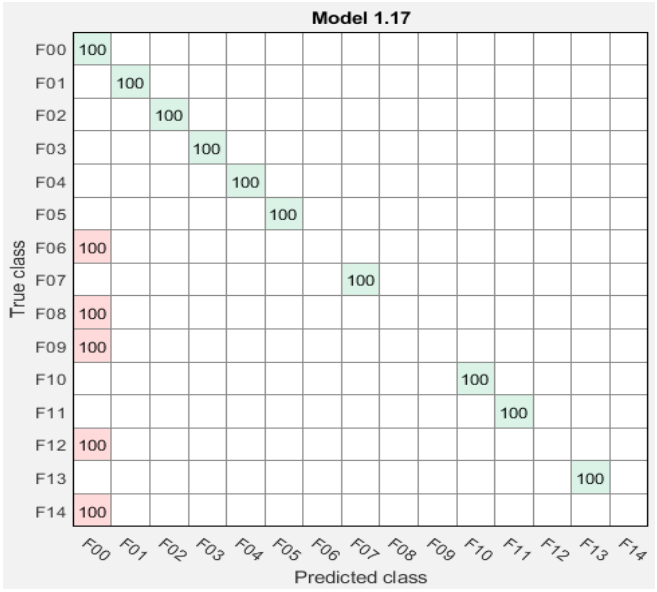

Fig. 23. Confusion matrix of weighted KNN classifier with no validation.

IV. Results and discussion

Figures 7 to 14 show that the investigated faults can be classified into two types: detected and non detected faults. Therefore, ambiguous fault groups are constructed as illustrated in the tables III and IV. The letter D means a detected fault though ND stands for non detected fault.

Results presented in table III sum up the significant points in the frequency domain as follows:

- All bridging faults injected in CMOS operational amplifier have been detected using supply current and its phase responses.
- In the band pass Sallen&Key filter, 100% of these faults were detected using the supply current response, and 75% of faults were covered using the supply current phase response.

Table III
Bridging faults detection and ambiguous groups in frequency domain

Fault code	CMOS opamp			Sallen-Key band pass filter		
	gain	phase	Group G/ph	gain	phase	Group G/ph
F0	-	-	0	-	-	0
F1	D	D	1/1	D	D	1/1
F2	D	D	2/2	D	D	2/2
F3	D	D	3/3	D	D	3/3
F4	D	D	4/4	D	D	4/4
F5	D	D	5/5	D	D	5/5
F6	D	D	6/6	D	ND	6/0
F7	D	D	7/7	D	D	7/7
F8	D	D	8/8	D	ND	8/0
coverage	100%	100%		100%	75%	

Table IV
Open faults detection and ambiguous groups in frequency domain

Fault code	CMOS opamp			Sallen-Key band pass filter		
	gain	phase	Group G/Ph	gain	phase	Group G/Ph
F00	-	-	0	-	-	0
F01	D	D	1/1	D	D	1/1
F02	D	D	1/1	D	D	1/1
F03	D	D	3/3	D	D	3/3
F04	D	D	3/3	D	D	3/3
F05	D	D	5/5	D	D	5/5
F06	ND	ND	0/0	ND	ND	0/0
F07	D	D	7/7	D	D	7/7
F08	ND	ND	0/0	ND	ND	0/0
F09	ND	ND	0/0	ND	ND	0/0
F10	D	D	10/10	D	D	10/10
F11	ND	ND	0/0	ND	ND	0/0
F12	ND	ND	0/0	ND	ND	0/0
F13	D	D	13/13	D	D	13/13
F14	ND	ND	0/0	ND	ND	0/0
Coverage (%)	57.14	57.14		57.14	57.14	

From the table IV, the fault coverage ratio has attained 57.14% for all open faults injected in both the two circuits under test. In this case, six faults (F06, F08, F09, F11, F12, and F14) modeled as open gates, were not detected and creating an ambiguity group with F0. In this step, faults creating ambiguity can be distinguished using a method for fault classification based on machine learning algorithms, discussed in section III.

In terms of classification, the bridging fault's classes are classified with high accuracy equal to 100%, as reported in figure 18. This is a sign of the results improvement, as mentioned at the beginning of this section.

The classification results provided by the corresponding confusion matrixes depicted in figures 21, 22, and 23 clearly indicated that undetected open faults in section II can be dispatched between themselves. This is due to their different classification accuracy and false negative's parameters values as is the case of the F11 fault, which was classified with 100% accuracy, as shown in figure 23.

TABLE V
Classifiers accuracies for features combinations and 3 types of validation

Features combinations	classification accuracy		
	Cross validation (5 folds)	Holdout validation (25%)	No validation
All features	Linear SVM 62.5%	Linear SVM 63.2%	Weighted KNN 66.7%
P1, P2,P3, P4	57.5%	58.9%	60%
P5, P6, P7, P8	62.9%	63.7	**66.7%**
P1, P2, P5, P6	56.9%	57.6%	60%
P1, P2, P7, P8	**63.3%**	63.2%	66.7%
P3, P4, P5, P6	57%	57.6%	60%
P3, P4, P7, P8	63.2%	**64%**	**66.7%**
P1, P3, P5, P7	56.9%	57.3%	60%
P2, P4, P6, P8	62.8%	63.7%	**66.7%**

V. Conclusion

In this research work, a method based on supply current verification was carried out for the purpose of detecting and classifying faults in analog circuits built with CMOS operational amplifiers. The proposed testing approach has the advantage of high fault coverage and a low test time, and its merit is due to the use of the test technique based on the quiescent supply current. This method's efficiency has been validated through the test process of the CMOS operational amplifier and the Sallen-Key band pass filter, both working under open and bridging faults explored as single type ones.

The results of the experiments demonstrated the usefulness of the supply current testing method for the case of bridging faults, achieving 100% classification accuracy. However, some open faults that affected the transistors gates, either escaped or masking each other in this test type. For this raison, different machine learning classifiers have been used to increase the fault detection resolution and make these faults distinguishable from each other. This is made possible by measuring the different performances by mean of the confusion matrices evaluating tools for each classifier, as shown in table VI. As a result, the fault coverage rate was improved, going from 57.14% to

Table VI
Parameters of Undetected Faults Classes Issue from Confusion Matrices

Fault code	Accuracy (%)			Precision (%)			Sensitivity (%)			Specificity (%)		
	Fig. 21	Fig. 22	Fig. 23	Fig. 21	Fig. 22	Fig. 23	Fig. 21	Fig. 22	Fig. 23	Fig. 21	Fig. 22	Fig. 23
F00	5	6	100	10.87	12.76	16.66	5	24	100	97.07	88.28	100
F06	8	0	0	8.60	0	0	8	0	0	94.67	99.71	100
F08	6	8	0	10	66.67	0	6	8	0	96.19	99.71	100
F09	7	20	0	7.45	11.36	0	7	20	0	93.78	88.85	100
F11	91	88	100	71.65	70.97	100	91	88	100	97.37	97.41	100
F12	19	16	0	11.73	11.43	0	19	16	0	89.78	91.14	100
F14	14	4	0	11.86	7.14	0	14	4	0	92.04	96.28	100

66.7%. Despite this small leap of improvement, fault classes F0 and F11 joined the list of detected faults with 100% classification accuracy. Other faults are also distinguishable by referring to the performance of the confusion matrices as presented in table VI.

As a perspective work, attention will be paid to finding efficient test parameters which contribute to the improvement of the accuracy of the classifier while increasing the detection rate of open circuit faults of the CMOS operational amplifier.

Acknowledgment

This research has been supported by the Algerian ministry of higher education and scientific research (research project, PRFU N°: A10N01UN100120220001).

References

[1] S. Franco, "Analog circuit design discrete and integrated", *in Electrical and Computer Engineering*, 1st edition, New York: McGraw-Hill Series, 2015, pp 488-500.

[2] P. Kakoty, " Design of a high frequency low voltage CMOS operational amplifier", *International Journal of VLSI design & Communication Systems (VLSICS)*, vol. 2, no.1, March 2011.

[3] A. Sadeqi, J. Rahmani, S. Habibifar, "Design Method for Two-Stage CMOS Operational Amplifier Applying Load/Miller Capacitor Compensation", *Computational Research Progress in Applied Science & Engineering, CRPASE: Transactions of Electrical, Electronic and Computer Engineering*, 6 (2020) 153–162.

[4] R. Kumar, "Design of Two Stage CMOS Operational Amplifier", *International Journal of Science and Research (IJSR)*, vol.10, no. 6, June 2021, pp 1505-1508.

[5] A. Arabi, N. Bourouba, A. Belaout and M. Ayad, "An accurate classifier based on adaptive neuro-fuzzy and feature selection techniques for fault classification in analog circuits," *Integration: the VLSI Journal*, vol. 64, pp. 50-59, 2019.

[6] M. Karmani, C. Khedhiri, B. Hamdi, B, Bensalem, "A Fault Dictionary-Based Fault Diagnosis Approach for CMOS Analog Integrated Circuits", *International Journal of VLSI design & Communication Systems (VLSICS)*, vol. 2, no .3, September 2011.

[7] S. M. Ishraqul Huq, B. A. Bhuiyan, M. Ahmed, "Investigating the Effectiveness of Current Monitoring Methods to Detect Bridging and Stuck-Open Faults in CMOS Circuits", *IOSR Journal of VLSI and Signal Processing*, vol. 10, no. 4, pp. 01-07, 2020.

[8] J. Font, R. Picos, M. Roca, E. Isern, E E, "A new BICS for CMOS operational amplifiers by using oscillation test techniques", *Microelectronics Journal,* 34 (2003), pp 919–926.

[9] J. Font, J. Ginard, E. Isern, M. Roca, J. Segura and E. Garcia, "Oscillation-Test Technique for CMOS Operational Amplifiers by Monitoring Supply Current", *Analog Integrated Circuits and Signal Processing*, vol. 33, pp. 213–224, 2002.

[10] S. Yellampalli, A. Srivastava and V. K. Pulendra, "A combined oscillation, power supply current and I/sub DDQ/ testing methodology for fault detection in floating gate input CMOS operational amplifier"?, *48th Midwest Symposium on Circuits and Systems*, vol. 1, pp. 503-506, 2005.

[11] J. S. Kumar, A. Deepthi, U. Kaveri, N. R. Sharma, "Assessment on the Adequacy of Current SupplyTesting Methods in CMOS Operational Amplifier", *International Journal of Engineering and Advanced Technology (IJEAT)*, vol. 9, no 5, pp. 296-299, June 2020.

[12] M. Kaur, J. Kaur, "IDDQ Testing of Low Voltage CMOS Operational Transconductance Amplifier", *International Journal of Electrical and Computer Engineering (IJECE)*, vol. 8, no. 3, pp. 1467-1477, June 2018,

[14] C. L. Hsu, M. H. Ho and C. F. Lin, "Novel Built-In Current-Sensor-Based IDDQ Testing Scheme for CMOS Integrated Circuits," *in IEEE Transactions on Instrumentation and Measurement*, vol. 58, no. 7, pp. 2196-2208, July 2009.

[15] B. Guibane, B. Hamdi, A. Mtibaa, "Investigation on the effectiveness of current supply testing methods in CMOS operational amplifiers", *15th International Multi-Conference on Systems, Signals & Devices (SSD)*, 2018, pp. 1041-1044.

[16] B. Esen, A. Coyette, G. Gielen, W. Dobbelaere and R. Vanhooren, "Effective DC fault models and testing approach for open defects in analog circuits," *IEEE International Test Conference (ITC)*, pp. 1-9, 2016.

[17] M. Merabet and N. Bourouba, "DC Hard Faults Detection and Localization in Analog Circuits Using Fuzzy Logic Techniques", *Electronics journal*, vol. 23, no. 1, pp. 18-25, JUNE 2019.

[18] M. Tadeusiewicz, S. Hałgas, "Multiple soft fault diagnosis of DC analog CMOS circuits designed in nanometer technology", *Analog Integr Circ Sig Process*, vol.88, pp. 65–77, 2016.

[19] C. Wannaboon, N. Jiteurtragool1, W. San-Um, M. Tachibana, "Phase difference analysis technique for parametric faults BIST in CMOS analog circuits", *IEICE Electronics Express*, vol.15, no.9, pp. 01–09, 2018.

[20] S. Thakur, "A Complete Monte Carlo and Sensitivity Analysis of Various Elements in Analog VLSI Circuits", *International Journal of u- and e-Service, Science and Technology*, vol. 9, no. 11, pp.239-250, 2016 .

[21] A. Kulkarni, D. Chong, F. A. Batarseh, "Foundations of data imbalance and solutions for a data democracy", *Data Democr*, pp. 83-106, 2020. https://doi.org/10.1016/B978-0-12-818366-3.00005-8.
W. M. Salilew, Z. A. Abdul Karim, T. A. Lemma, "Investigation of fault detection and isolation accuracy of different Machine learning techniques with different data processing methods for gas turbine", *Alexandria Engineering Journal*, vol. 61, no. 12,pp. 12635-12651, 2022.